

Mars: Northern hemisphere slopes and slope distributions

Oded Aharonson, Maria T. Zuber¹, Gregory A. Neumann¹

Department of Earth, Atmospheric and Planetary Sciences, Massachusetts Institute of Technology, Cambridge, Massachusetts

James W. Head III

Department of Geological Sciences, Brown University, Providence, Rhode Island

Abstract. We investigate slope distributions in the northern hemisphere of Mars from topographic profiles collected by the Mars Orbiter Laser Altimeter. Analysis of the region from about 12°S to 82°N, over diverse geologic units, indicates that the range of regional-scale slopes is small, generally < 3°. Surface smoothness is most distinctive in the vast northern hemisphere plains, where slopes are typically < 1°. Amazonis Planitia is particularly remarkable in its smoothness, exhibiting an rms variation in topography of < 2 m over a 100-km baseline. This relative smoothness is still present when compared with other sampled areas of the Martian northern hemisphere and with volcanically resurfaced terrains elsewhere in the solar system. Planetary surfaces of large areal extent that are most comparable to Amazonis in terms of rms elevation variation over long baselines are depositional in origin and include terrestrial oceanic abyssal plains and certain sedimentary basins. Slopes across the Valles Marineris canyon system show that the upper portion of the walls are significantly and consistently steeper than the lower walls, characteristic of extensive mass wasting. The observed long-runout is consistent with a high-energy collapsed flow. In the neighboring Noctis Labyrinthus canyons the duality between the upper and lower walls is reduced, and indicates a lower energy modificational history and/or greater cohesion of wall rock.

Introduction

Slopes and their statistical distribution are useful descriptors of planetary surfaces in that they can be pertinent to the mechanisms of formation of physiographic features, and are indicative of the style and duration of subsequent modificational processes. As a step towards quantifying the nature of surface processes of Mars, we analyze slope distributions derived from topographic profiles of the northern hemisphere from the Mars Orbiter Laser Altimeter (MOLA) [Zuber *et al.*, 1992], an instrument on the Mars Global Surveyor (MGS) spacecraft. The profiles were collected during orbital periapses 3 and 20 through 36 during the MGS capture orbit and aerobreaking hiatus periods in September-November, 1997 [Albee *et al.*, 1998]. The data have a 300-

400-m resolution along track, a 1200-km separation across track, a range resolution of 37.5 cm, a range precision of 1-10 m for surface slopes of up to 30°, and an absolute accuracy of 30 m with respect to Mars' center of mass [Smith *et al.*, 1998]. These data currently constitute the highest quality measurements of Mars topography and permit quantification of slopes from local to hemispheric scale.

In this analysis surface slopes from MOLA observations were obtained over a ~ 600 m baseline from a 3-point Lagrange slope formula applied along track, and on longer baselines (> 10 km) from fitting a line to a set of points along a track. Slope properties and statistics have been examined and contrasted on various planetary surfaces (see for example *Sharpton and Head, 1985*).

Local and Regional Slopes

Figure 1 shows mean slopes on a 10-km baseline calculated by line fitting for selected passes. A number of deductions can be made upon closer examination of slopes over various baselines.

Subtle though notable long wavelength slopes are displayed in association with the massive volcano-tectonic Tharsis rise. Tharsis-related volcanic units rise gently (Figure 1, pass 24) for 2500 km at 0.08°, with a root mean square (rms) deviation from a flat sloping surface of only 61 m. Olympus Mons, the largest known volcano in the solar system, displays comparable flank slopes (~ 2.5 – 5°) to Hawaiian shields (Figure 2). Abrupt changes in slope are apparent in the marginal scarp of Olympus Mons, at the headwalls of the aureole deposits, where the slope is ~ 19°, but can approach 30° if calculated over the shortest baselines observed.

The hemispheric dichotomy boundary region, which separates the low, volcanically resurfaced northern hemisphere from the older, heavily cratered and topographically higher southern hemisphere [Carr, 1981] rises upwards toward the south from about -4 km to 2 km over ~ 400 km distance, giving less than a 1° mean slope. However, in some passes in the eastern hemisphere of Mars, the boundary is observed to have slopes on short baselines exceeding 20° (see also *Frey et al.*, this issue). Topographic roughness along the boundary on 10-km baselines is comparable to that in the southern highlands, though slopes along the boundary region have been influenced significantly by tectonic and erosional processes in addition to impact, which dominates in the south.

A set of features that display complexly varying local slopes are the canyon systems. Figure 3 shows the topogra-

¹Also at: Laboratory for Terrestrial Physics, NASA Goddard Space Flight Center, Greenbelt, Maryland.

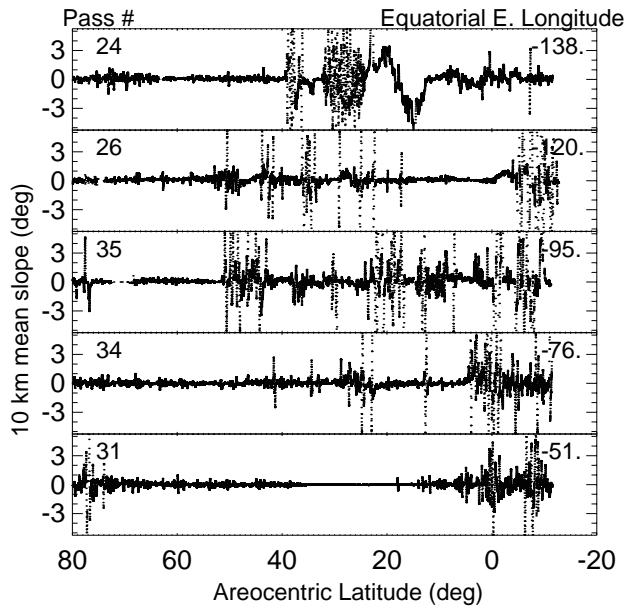


Figure 1. 10-km mean slopes across Mars' northern hemisphere for MOLA Passes 24,26,35,34, and 31.

phy and associated slopes across the largest of these systems, Valles Marineris (VM). Here local (600-m) slopes range from essentially flat over the valley floors, to typically less than 5° at the lower canyon walls, to 28° at the upper walls. Such a distribution indicates extensive mass wasting related to the slumping and erosion of material from the upper walls, which leaves behind a scarp that can expose bedrock. When slopes are observed as function of height above the valley floor, the lower 20% of the wall never exceeds $\sim 18^\circ$ while the upper 30% of the wall almost never drops below $\sim 20^\circ$. Downslope material transport can occur by rotational listric faulting, mass wasting of individual fragments, talus formation, and landslides. The distance over which transported material is distributed across the valley floor is indicative of the energy of the transport process and the competence of canyon wall material. Across VM talus slopes extend to tens of km across the valley floor [Lucchitta, 1992], which implies high energy and/or low effective friction of the mass movement [McEwen, 1989]. In contrast, the correlation between elevation and slope angle is much weaker in Noctis Labyrinthus, which marks the summit region of the Tharsis rise and forms the western-most component of the VM canyon system. Figure 3 shows that the Noctis chasmata are steeper on the lower extent of the canyon walls and have apparently undergone less mass wasting than in central VM. A chasm on Elysium rise ($22.25^\circ\text{N } 141.5^\circ\text{E}$) [Smith et al., 1998] shows a correlation between slope and wall elevation that is distinctive from but more comparable to the Noctis chasmata than to central VM chasmata. These observations provide an initial indication of the variability of erosional intensity or near surface cohesion that can be quantified with future observations.

Regional Roughness

The topographic distribution function is typically long-tailed due to cratering, faulting, and other localized pro-

cesses. We therefore quantify the regional roughness using the interquartile scale (IQS) variation of topography in a window of width 100-km along track. In this characterization we measure the width of a histogram of only the most significant 50% of the elevations, scaled to unity in the case of a normal distribution. Before normalization, this estimator R_q is defined [Neumann and Forsyth, 1995] as

$$R_q = \frac{N}{2N-1}(Q_3 - Q_1) \quad (1)$$

where Q_i is the elevation of the i^{th} quartile point and N is the number of points. To normalize, R_q is divided by 0.673, the IQS of a normal distribution. The parameter R_q is a robust estimator in the sense that it is not sensitive to outliers in as much as half of the population. We apply this calculation to all range returns that fall within a 100-km window sliding along the points on each profile. It is possible to detrend the points in a given window to remove the regional slope before calculating the IQS, but doing so proved to change none of the following characteristics that emerge distinctly from the analysis.

The northern hemisphere is surprisingly flat with typical inter-quartile scale of a few tens of meters, ranging over thousands of kilometers (*cf.* Zuber et al., this issue). The Olympus Mons aureole deposits are the roughest surfaces observed, with IQS exceeding 2 km. The most unusual region is Amazonis Planitia, an area to the northwest of Olympus Mons of Amazonian age and elevation of approximately -4.1 km relative to the average equatorial geoid. This surface displays an rms variation in topography of only a few meters (still above the instrument's range resolution), extending over hundreds of kilometers, and correlating well with previously mapped geology. The smoothest part of the surface corresponds to member 3 of the Arcadia Formation, which is interpreted to consist largely of lava flows and small volcanoes [Scott and Tanaka, 1986]. Member 3 also forms smooth plains west of the Olympus Mons aureoles and displays occasional flow fronts at Viking resolution. This area has an anomalously low thermal inertia (between 2 and 3×10^{-3} cal cm $^{-2}$ s $^{-1/2}$ K $^{-1}$ [Christensen and

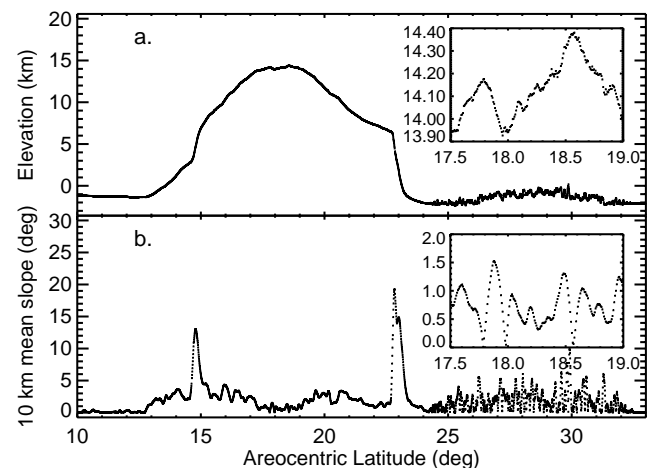


Figure 2. Topography (a) and slopes (b) across the Olympus Mons shield (Pass 24; longitude -138° E). A portion of the profile running west of the volcano's summit is shown in the insert.

Moore, 1992]) with very low variability over tens of km scale, anomalously low radar backscatter cross-section at a variety of wavelengths [Jakosky and Muhlemann, 1981], and has been interpreted to be accumulations of fine-grained dust [Christensen, 1986]. The regional flatness and low surface roughness detected by MOLA is consistent with this interpretation but does not uniquely explain the genesis of this region.

An initial step towards identifying the mechanism of formation of Amazonis Planitia is to compare its topographic properties to other smooth regions with potentially analogous origins. Shown in Figure 4 are profiles of elevation collected by various altimeters over smooth surfaces from a variety of solar system bodies. At the top is MOLA Pass 31 over Amazonis Planitia, where the anomalously smooth region is observed to extend over 600 km, approximately centered in the plot (vertical point-to-point accuracy $\delta z \sim 0.4$ m, horizontal resolution $\delta x \sim 0.3$ km). Below is a Clementine profile of the Moon's Oceanus Procellarum ($\delta z \sim 40$ m, $\delta x \sim 2$ km for 1 Hz data and ~ 0.2 km for 8 Hz data) [Smith et al., 1997], Magellan radar altimetry over Niobe Planitia ($\delta z \sim 4$ m, $\delta x \sim 10$ km) [Ford and Pettengill, 1992], Shuttle Laser Altimeter data collected over the Sahara desert ($\delta z \sim 1.5$ m, $\delta x \sim 0.7$ km) [Garvin et al., 1997], and shiptracks of Seabeam 2200 bathymetry over the south Atlantic abyssal plains ($\delta z \sim 2$ m, $\delta x \sim 0.1$ km) [Neumann et al., 1996]. The last two profiles were extracted from the GTOPO data set (highly variable $\delta z \sim 20$ m, $\delta x \sim 0.1$ km) [Gesch and Larson, 1996], first over the Great Plains in the U.S., and second over the Indo-Gangedic Plains across over the Tibetan Plateau, down across the Tarim Basin and continuing northwards. Oceanus Procellarum consists of lava flows that have been broadly tilted by subsidence and locally steepened by tectonic deformation (wrinkle ridges); their small-scale roughness is dominated by impact regolith formation processes. Niobe Planitia on Venus consists of vast lava plains similarly tilted and steepened but not influenced by regolith formation. Comparison of these surfaces reveals that of these lowest, smoothest regions observed in the solar system, Amazonis Planitia closely resembles in its smoothness only the heavily sedimented surfaces on the Earth, *i.e.*

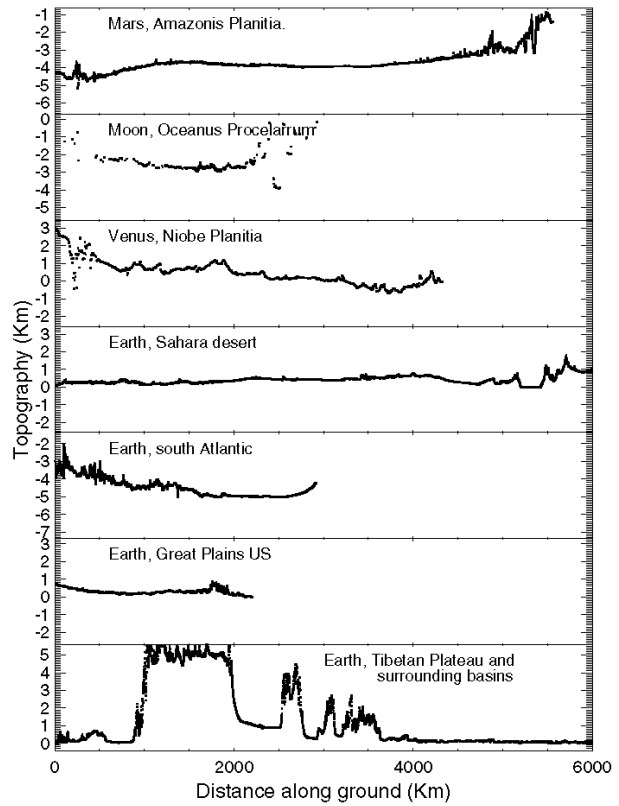


Figure 4. Comparison of planetary surface topography. See text for description.

oceanic abyssal plains and basins filled by fluvial deposition processes. It is noteworthy that volcanically resurfaced terrain is markedly rougher on the Moon, on Venus, and on Mars, than the peculiar Amazonis deposits. Saharan sand sheets are rougher by a factor of about three. Other regions in the Martian northern hemisphere that exhibit evidence of dust deposition are rougher than Amazonis as well.

Conclusions

Characterization of Martian surface slopes from the aerobraking hiatus phase of the MGS mission provided several insights. Regional slopes across prominent canyons measured on a 10-km baseline range from $0 - 5^\circ$ for regions which have undergone mass wasting and collapse, up to approximately 30° for less modified scarps. The average slopes across the dichotomy boundary are small, $< 1^\circ$, but on a local scale can exceed 20° . The northern lowlands are found to be unusually smooth and form a distinct statistical population. Other distinct populations correspond to the rough highlands and the extremely smooth Amazonis Planitia region. Amazonis is markedly smoother than any other large-scale surface observed on Mars, than volcanic plains on both the Moon and Venus, and than an example of desert terrain on the Earth. Its statistical properties resemble most closely certain terrestrial depositional environments including oceanic abyssal plains and sedimentary basins. Given previously hypothesized scenarios for Mars' geological past [Carr, 1981], the evidence so far may be consistent with an origin for Amazonis in which extensive aeolian deposition

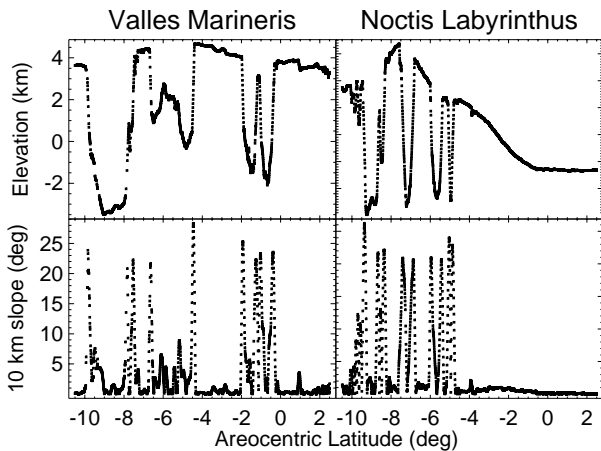


Figure 3. Topography and slopes across central Valles Marineris (Pass 35; longitude -77° E) and Noctis Labyrinthus (Pass 26; longitude -95° E).

follows a volcanic resurfacing event. Also possible is a modificational history in which water provides a sedimentary environment capable of efficiently smoothing meter scale topography.

Acknowledgments. We acknowledge helpful discussions with Kelin Whipple and Tom Jordan. This study was supported by the Mars Global Surveyor Project.

References

- Albee, A. A., F. D. Palluconi and R. E. Arvidson, Mars Global Surveyor Mission: Overview and status, *Science*, *279*, 1671-1672, 1998.
- Carr, M. H., *The Surface of Mars*, 232 pp., Yale University Press, New Haven, 1981.
- Christensen P. R., Regional dust deposits on Mars: Physical properties, age, and history, *J. Geophys. Res.*, *91*, 3,533-3,545, 1986.
- Christensen P. R. and H. J. Moore, The Martian Surface Layer, *Mars*, p. 686-729, ed. H. H. Kieffer, B. M. Jakosky, C. W. Snyder, and M. S. Matthews, Univ. of Ariz. Press, Tucson, 1981.
- Ford, P. G. and G. H. Pettengill, Venus topography and kilometer-scale slopes, *J. Geophys. Res.*, *97*, 13,103-13,114, 1992.
- Fox, C. G. and D. E. Hayes, Quantitative methods for analyzing the roughness of the seafloor *Rev. Geophys.*, *23*, 1-48, 1985.
- Frey, H. V, S. E. H. Sakimoto, and J. Roark, The MOLA Topographic signature of the crustal dichotomy boundary zone on Mars, *Geophys. Res. Lett.*, this issue, 1998.
- Garvin, J. B., J. L. Bufton, J. B. Blair, S. B. Luthcke, J. J. Frawley and J. A. Marshall, Observations of the Earth's topography from the Shuttle Laser Altimeter (SLA): Laser pulse echo recovery measurements of terrestrial surfaces, *Proc. European Geophys. Soc. Mtg.*, Vienna, 1997.
- Gesch, D.B., and Larson, K.S., Techniques for development of global 1-kilometer digital elevation models, *Pecora Thirteen, Human Interactions with the Environment - Perspectives from Space*, Sioux Falls, South Dakota, August 20-22, in press, 1996.
- Jakosky, B. M. and D. O. Muhleman, A comparison of the thermal and radar characteristics of Mars, *Icarus*, *45*, 25-38, 1981.
- Lucchitta, B. K., A. S. McEwen, G. D. Clow, P. E. Geissler, R. B. Singer, R. A. Schultz, and S. W. Squyres, The Canyon Systems of Mars, *Mars*, p. 453-492, ed. H. H. Kieffer, B. M. Jakosky, C. W. Snyder, and M. S. Matthews, Univ. of Ariz. Press, Tucson, 1981.
- McEwen, A. S, Mobility of Large Rock Avalanches: Evidence from Valles Marineris, Mars, *Geology*, *17*, 1111-1114, 1989.
- Neumann, G. A. and D. W. Forsyth, High resolution statistical estimation of seafloor morphology: Oblique and orthogonal fabric on the mid-Atlantic ridge, *Marine Geophys. Res.*, *17*, 221-250, 1995.
- Neumann, G. A., P. J. Michael and B. B. Hanan, Temporal variation of crustal emplacement, 33° S Mid-Atlantic Ridge, *J. Conf. Abs.*, *1*, 836-837, 1996.
- Scott, D. H., and K. L. Tanaka, Geologic Map of the Western Equatorial Region of Mars, Scale 1:15,000,000, *U.S. Geol. Survey Map I-1802-A*, 1986.
- Sharpton, V. L., J. W. Head III, Analysis of regional slope characteristics on Venus and Earth, *J. Geophys. Res.*, *90*, 3733-3740, 1985.
- Smith, D. E., M. T. Zuber, The shape of Mars and the topographic signature of the hemispheric dichotomy, *Science*, *271*, 184-188, 1996.
- Smith, D. E., M. T. Zuber, W. B. Banerdt, H. V. Frey, J. B. Garvin, J. W. Head III, D. O. Muhleman, G. H. Pettengill, R. J. Phillips, S. C. Solomon, H. J. Zwally, W. B. Banerdt, T. C. Duxbury, Topography of the northern hemisphere of Mars from the Mars Orbiter Laser Altimeter (MOLA), *Science*, *279*, 1686-1692, 1998.
- Smith D. E., M. T. Zuber, G. A. Neumann and F. G. Lemoine, Topography of the Moon from the Clementine lidar, *J. Geophys. Res.*, *102*, 1591-1611, 1997.
- Zuber, M. T., D. E. Smith, J. W. Head, R. J. Phillips, S. C. Solomon, G. A. Neumann, and O. Aharonson, The shape of the northern hemisphere of Mars from the Mars Orbiter Laser Altimeter (MOLA), *Geophys. Res. Lett.*, this issue, 1998.
- Zuber, M. T., D. E. Smith, S. C. Solomon, D. O. Muhleman, J. W. Head III, J. B. Garvin, J. B. Abshire, J. L. Bufton, The Mars Observer Laser Altimeter investigation, *J. Geophys. Res.*, *97*, 7781-7797, 1992.

O. Aharonson, G. A. Neumann and M. T. Zuber, Department of Earth, Atmospheric and Planetary Sciences, Massachusetts Institute of Technology, Cambridge, MA 02139 (e-mail: oded@mit.edu)

J. W. Head III, Department of Geological Sciences, Box 1846 Brown University, Providence, RI 02912

(Received June 22, 1998; revised September 1, 1998; accepted September 17, 1998.)